

Hydrodynamic analysis of a TLP platform with cables and cable lay-outing

Auteur : Karyaparamban, Abdul Fathah

Promoteur(s) : 14928

Faculté : Faculté des Sciences appliquées

Diplôme : Master : ingénieur civil mécanicien, à finalité spécialisée en "Advanced Ship Design"

Année académique : 2020-2021

URI/URL : <http://hdl.handle.net/2268.2/13640>

Avertissement à l'attention des usagers :

Tous les documents placés en accès ouvert sur le site le site MatheO sont protégés par le droit d'auteur. Conformément aux principes énoncés par la "Budapest Open Access Initiative"(BOAI, 2002), l'utilisateur du site peut lire, télécharger, copier, transmettre, imprimer, chercher ou faire un lien vers le texte intégral de ces documents, les disséquer pour les indexer, s'en servir de données pour un logiciel, ou s'en servir à toute autre fin légale (ou prévue par la réglementation relative au droit d'auteur). Toute utilisation du document à des fins commerciales est strictement interdite.

Par ailleurs, l'utilisateur s'engage à respecter les droits moraux de l'auteur, principalement le droit à l'intégrité de l'oeuvre et le droit de paternité et ce dans toute utilisation que l'utilisateur entreprend. Ainsi, à titre d'exemple, lorsqu'il reproduira un document par extrait ou dans son intégralité, l'utilisateur citera de manière complète les sources telles que mentionnées ci-dessus. Toute utilisation non explicitement autorisée ci-avant (telle que par exemple, la modification du document ou son résumé) nécessite l'autorisation préalable et expresse des auteurs ou de leurs ayants droit.



Universitäts
Rostock



Traditio et Innovatio



SOLENT
UNIVERSITY
SOUTHAMPTON



Zachodniopomorski
Uniwersytet
Technologiczny
w Szczecinie



With the support of the
Erasmus+ Programme
of the European Union

GICON[®]
Gruppe

Hydrodynamic Analysis of a TLP platform with Cables and Cable Lay-outing

submitted on 13 August 2021

Submitted by KARYAPRAMBAN Abdul Fathah

Address: Darusalam House, Kodangadu, Kondotty (P.O.), 673638, India

Email: Abdul-Fathah.Karyaparamban@eleves.ec-nantes.fr

Student ID No.: 200549H

First Reviewer:

Felicien Bonnefoy

Maître de conférences

Ecole Centrale Nantes (ECN)

1 rue de la Noe

44321 Nantes, France

Second Reviewer:

Vincent Leroy

Maître de conférences

Ecole Centrale Nantes (ECN)

1 rue de la Noe

44321 Nantes, France



TABLE OF CONTENTS

LIST OF FIGURES.....	4
LIST OF TABLES	5
1 ABSTRACT.....	7
2 INTRODUCTION.....	8
3 THEORETICAL BACKGROUND	9
3.1 Large Volume Structures.....	9
3.2 Morison elements	11
3.3 Time Domain Dynamic Simulation.....	12
4 STATE OF THE ART REVIEW OF AC/DC & PLATFORM WINDFARM CABLING	
14	
4.1 Typical Offshore Wind Farm Arrangement	14
4.2 Electric Cable	14
4.3 Factors Influencing the Design of Optimal Cable Path.....	16
4.4 Components in Cable Lay-outing.....	18
4.4.1 Cable buoy.....	18
4.4.2 Dynamic Cable Bending Stiffeners.....	18
4.4.3 Cable Bending Resistor.....	19
4.4.4 J or I tube.....	19
4.4.5 Burial and Non-burial of Cables at Sea bed.....	20
4.4.6 Cable Hang-offs	21
4.4.7 State-of-art-review for Hydrodynamic Analysis of TLP platforms	22
5 METHODOLOGY AND RESULTS FOR HYDRODYNAMIC ANALYSIS OF TLP.	25
5.1 Co-ordinate System Used in ANSYS Aqwa	26
5.2 Environment Loads.....	26

5.2.1	Regular Wave, Wind and Current – Regular Wave ULS	26
5.2.2	Irregular Wave, Wind and Current - Irregular Wave ULS	26
5.3	Mass Properties of Platform	27
5.4	Hydrodynamic Modeling of Geometry	27
5.5	Hydrodynamic Diffraction (HD) Analysis	30
5.6	Mooring Lines Properties	31
5.6.1	Calculation of Pretension & Unstretched length of the Tendons.....	32
5.7	Stability Analysis.....	32
5.8	Hydrodynamic Response (HR) Analysis.....	33
5.8.1	Current Drag Coefficient Calculation	33
5.8.2	Wind Drag Coefficient Calculation.....	38
5.8.3	Response Analysis for Maximum Regular Wave Height	39
5.8.4	Response Analysis for Irregular Wave (ULS)	41
5.9	Cable Lay-outing	43
5.9.1	Cable and Buoy properties	44
5.9.2	Cable Arrangement and Shapes	44
5.9.3	Cable Tension.....	44
6	CONCLUSION	46
7	FUTURE WORK	47
8	ACKNOWLEDGEMENT	48
9	REFERENCE	49

LIST OF FIGURES

Figure 1: Definition of normal and tangential force on Morison element	12
Figure 2: A typical offshore wind farm energy transport diagram (W.-S.Moon, 2014).....	14
Figure 3: Typical 3-Phase AC subsea power cable cross section (DNVGL-ST-0359, June, 2016).....	15
Figure 4: Cable armour. (a) Z- and S- lay, (b) forces, (c) unbalanced armour, (d) torsion balanced armour (DNV-RP-J301, 2016).....	15
Figure 5: Cable connection between wind turbine and substation – lazy wave shape.....	17
Figure 6: Cable connection on floating structure – lazy wave with wire (TANINOKI, 2017).....	17
Figure 7: Cable buoy	18
Figure 8: Bend stiffeners	18
Figure 9: Cable bending resistor (*).....	19
Figure 10: Elevated section view of cable bending resistor (**)	19
Figure 11: “I”-tube section.....	20
Figure 12: Various burial condition of cable at sea bed (DNV-RP-J301, 2016)	21
Figure 13: Various non-burial condition of cable at sea bed (DNV-RP-J301, 2016).....	21
Figure 14: Typical design of the cable hang-off (DNV-RP-C205, 2010).....	22
Figure 15: Semi-Submersible Platform mooring and cabling arrangement.....	24
Figure 16: Spar Platform mooring and cabling arrangement.....	24
Figure 17: TLP mooring and cabling arrangement	24
Figure 18: Steps used for hydrodynamic analysis of TLP	25
Figure 19: Direction of Wave/Wind/current	26
Figure 20: Different wave force regimes (DNV-RP-C205, 2010) (H: Wave height, D: characteristic dimension).....	28
Figure 21: Drag coefficient for circular cylindrical section for various Re and roughness (k), (DNV-RP-C205, 2010)	35
Figure 22: Wake amplification factor as function of Kc number for smooth (solid line- $C_{DS} = 0.65$) and rough (dotted line- $C_{DS} = 1.05$) (DNV-RP-C205, 2010).....	36
Figure 23: Orientation of rectangular cross section against the current.....	37
Figure 24: Catenary shape-dimensions	44
Figure 25: Lazy wave shape-dimensions	44

LIST OF TABLES

Table 1: Tendon's properties.....	31
Table 2: Co-ordinate of mooring end points	31
Table 3: Natural period and damping ratio	32
Table 4: Drag coefficient of rectangular cross section (DNV-RP-C205, 2010)	37
Table 5: Wind drag coefficient.....	38
Table 6: Drag coefficient for new structure	42
Table 7: Mooring line tension for irregular wave case – For modified structure	42
Table 8: Electrical cable and Buoy properties	44
Table 9: Maximum and minimum tension of cables at the floater connection	45

DECLARATION OF AUTHORSHIP

I declare that this thesis and the work presented in it are my own and have been generated by me as the result of my own original research.

Where I have consulted the published work of others, this is always clearly attributed.

Where I have quoted from the work of others, the source is always given. With the exception of such quotations, this thesis is entirely my own work.

I have acknowledged all main sources of help.

Where the thesis is based on work done by myself jointly with others, I have made clear exactly what was done by others and what I have contributed myself.

This thesis contains no material that has been submitted previously, in whole or in part, for the award of any other academic degree or diploma.

I cede copyright of the thesis in favour of the University of the Ecole Centrale de Nantes.

Date: 12/08/2021

Signature:

A handwritten signature in black ink, consisting of a series of loops and a long horizontal stroke at the end, written over a diagonal line.

1 ABSTRACT

The report focuses on the state-of-the-art review of AC/DC Tension Leg Platform (TLP) cable lay-outing and hydrodynamic modelling & analysis of the GICON AC/DC TLP platform in ANSYS Aqwa. GICON AC/DC TLP platform is designed by the conversion of existing GICON O&M Platform. The platform is analyzed for 100-year return period irregular ($H_s=13.54$ m, $T_p=13.89$ s) and regular wave ($H_{max} = 25.26$ m, $T = 13.89$ sec) in North Atlantic Sea having 200m water depth case. The mass properties of the platform (such as center of gravity, weight and mass moment of inertia about center of gravity) are calculated using the software, SOLIDWORKS. The viscous drag forces are approximated using analytical equations as per (DNV-RP-C205, 2010).

The maximum offset of the platform, angle of the mooring lines with vertical, maximum tension on mooring lines, relative distance between wave surface and cable deck, relative distance between wave surface and bottom of the pontoon are checked for both regular and irregular wave severe conditions. To satisfy the design criteria, TLP platform geometry has been modified and ensured the design limits within the criteria for the modified structure.

Two basic configurations of electrical cable are modelled – catenary and lazy wave shape. Cable tension due to the motion of the floating structure at the connection of platform with electrical cable are compared and chose the best configuration for the AC/DC TLP platform.

2 INTRODUCTION

To bring world to a better place, energy sectors are moving from oil industry to renewable energy sectors. One of the main renewable energy sources is energy production utilizing wind energies. By using large scale series production methods, larger wind turbines with extended full load hours for floating offshore installations could result in reduced levelized costs. To reduce the visual impact from the shore, such wind turbines have to be installed in deeper waters with depth greater than 60m. As the wind farm is far from the shore, extensive infrastructure in the form of further platforms for maintenance, power conversion and/or energy storage must be provided.

There are two type of offshore platform designs – fixed and floating. Floating platforms are more economical in deep sea (greater than 60 m) compared to fixed foundations. Also, as the floating wind parks are far away from the shore, the cost for access/maintenance of the park will be huge. To mitigate this issue, GICON designed an operation and maintenance (O&M) TLP platform near the park. The objective of the report is to convert the existing O&M platform to AC/DC TLP platform to handle the electricity produced in the park and to transfer the electricity to the shore in most efficient way.

In actual case study, for the complete design of the floating platform includes the stability calculation for transportation, installation, operation condition of the platform, structural calculations, weight estimation etc. But this report focuses on the hydrodynamic analysis of the GICON AC/DC TLP platform (which is modified from the existing GICON Operation and Maintenance (O&M) TLP platform) for 100-year return period Ultimate Limit State (ULS) conditions – Regular and Irregular wave conditions which will be always the most unfavorable condition for a floating structure. For this purpose, a numerical model based on potential theory is modeled in ANSYS Aqwa. The report depicts the detailed hydrodynamic modeling and analysis of AC/DC TLP platform with electrical cables.

The main objective of the report is the state of art review of AC/DC Tension Leg Platform & wind farm cabling arrangement, Hydrodynamic analysis of the TLP platform with cables and cable layouts in ANSYS Aqwa and tension on electrical cable (at the connection of the platform and cable) and selection of the best cable lay-out shape. The fatigue strength of the

cable and consideration of the loads due to vortex induced vibration (VIV) are out of the scope of the report.

3 THEORETICAL BACKGROUND

Three-dimensional panel methods are the most common used numerical tool for hydrodynamic analysis of the large volume structures in waves. These methods are based on the fluid potential theory and represent the structure surface by a series of diffraction panels. The Morison's equation approach is widely used for slender body components. Aqwa employs a hybrid method to model the large-volume components of a structure by diffracting panels and the small cross-sectional components by Morison elements (ANSYS, 2013).

The mooring analysis of floating structure and it's cabling layout design has been carried out using potential solver, ANSYS Aqwa. The main assumption of the potential theory are fluid is inviscid, incompressible and fluid flow is irrotational. By using this assumption, the fluid flow can be represented by a potential function, ϕ .

$$\phi(\bar{X},t) = a_w e^{-i\omega t} \quad (1)$$

Here, a_w is the wave amplitude and ω is wave frequency. $\phi(\bar{X},t)$ is space and time dependent variable.

3.1 Large Volume Structures

If the structural size is same order as that of wave amplitude, the structure can be considered as large volume structures. Or Keulegan-Carpenter number ($Kc = 2\pi \frac{A}{D}$; where A is wave amplitude and D is size of the structure) is less than 2, the structure can be considered as large. If the $Kc > 10$, the structure will be considered as slender or Morison element. The large volume structure will be inertia dominated.

The entire floating first order potential problem can be divided in to incident, scattered and radiation potential;

$$\phi^{(1)} = \phi^I + \phi^S + \phi^R = \phi^D + \phi^R \quad (2)$$

And the radiation potential can further decompose by

$$\Phi^R = \sum_{k=1}^6 \Phi_k^R \xi_k \quad (3)$$

Here, k is the degrees of freedom (3 translational and 3 rotational degrees of freedom of the floating structure). ξ_k is the motion amplitude in degrees of freedom, k.

The potential must also satisfy the Laplace equation in addition to the boundary conditions;

$$\nabla^2 \Phi^{D,R} = 0 \quad (4)$$

$$\frac{\partial^2 \Phi^{D,R}}{\partial t^2} + g \frac{\partial \Phi^{D,R}}{\partial z} = 0, \quad \text{at } z=0 \quad (5)$$

$$\frac{\partial \Phi^D}{\partial n} = 0, \quad \text{on } S \quad (6)$$

$$\frac{\partial \Phi_f^D}{\partial n} = 0, \quad \text{on } S \quad (7)$$

Here, n is the unit vector normal to the floating wetted surface, S. There will be radiation and seabed boundary condition in addition to the above-mentioned boundary conditions. The system of equation can solve by Boundary Element Method, thanks to the of Green's function.

When the wave velocity potential is known, the first order hydrodynamic pressure on the structure can estimate using the following equation;

$$P^{(1)} = -\rho \frac{\partial \Phi(\bar{X}, t)}{\partial t} \quad (8)$$

Total first order hydrodynamic force can find out by surface integration of the above equation over the wetted surface of the floating structure.

The harmonic response of the structure for the unit wave amplitude regular wave (or Response Amplitude Operator) can be estimated using the equation;

$$[-\omega^2(M_s + M_a) - i\omega C + K_{hys}][x_{jm}] = [F_{jm}] \quad (9)$$

Here, M_s is the 6x6 mass matrix, M_a is the 6x6 added mass matrix and C is the damping matrix. K_{hys} is the hydrostatic stiffness matrix of the structure. If structure is moored, the mooring stiffness can be added in addition to hydrostatic stiffness.

Evaluation of the second order force is one of the major concerns in hydrodynamic analysis. Under the assumption of fluid amplitude and structural motions are small, using perturbation approach and Taylor series, the second order force can be approximated. Using perturbation approach, the velocity potential can be written as,

$$\phi = \varepsilon\phi^{(1)} + \varepsilon^2\phi^{(2)} + O(\varepsilon^3) \quad (10)$$

Here, (1) and (2) are first and second order variations with respect to perturbation parameter, ε .

3.2 Morison elements

For slender structures, the major force acting on the structure will drag force (drag dominated) compared to inertia load.

For slender structural members having cross-sectional dimensions sufficiently small to allow the gradients of fluid particle velocities and accelerations in the direction normal to the member to be neglected, wave loads may be calculated using Morison's load formula being a sum of an inertia force proportional to acceleration and a drag force being proportional to the square of velocity (DNV-RP-C205, 2010).

The drag coefficient C_D is non-dimensional drag force,

$$C_D = \frac{f_{drag}}{\frac{1}{2}\rho D v^2} \quad (11)$$

Here, f_{drag} : sectional drag force (N/m)

ρ : fluid density (kg/m³)

D : Characteristic dimension (m)

v : Velocity (m/s)

The drag force will be the resultant of the drag force in normal and tangential direction as shown in the Figure 1.

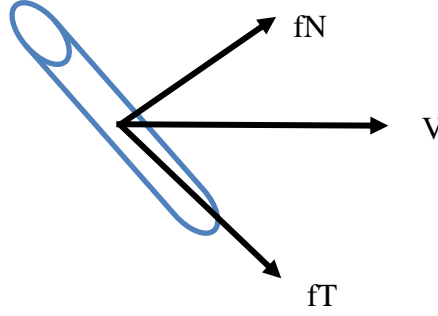


Figure 1: Definition of normal and tangential force on Morison element

Total force will be the sum of the force acting on each section along the length of the member. The sectional normal force can be written as,

$$f_N(t) = -\rho C_A A \ddot{r} + \rho(1 + C_A) A \dot{v} + \frac{1}{2} \rho C_D D v_r |v_r| \quad (12)$$

Where, C_A : Added mass coefficient

A : Cross-section area of the section (m²)

\ddot{r} : Acceleration of the member normal to the axis (m/s²)

\dot{v} : Fluid acceleration (m/s²)

v_r : Relative velocity between fluid and structure, $(v - \dot{r})$ (m/s²)

The sectional tangential force will be,

$$f_T(t) = \frac{1}{2} \rho C_{Dt} D v^2 \quad (13)$$

Here, C_{Dt} : tangential drag coefficient

3.3 Time Domain Dynamic Simulation

In time domain simulation, the position and velocity of the moored floating structure is determined at each time step by integrating the acceleration which will be found out using a two-stage predictor-corrector numerical integration scheme.

If the external force $F(t)$ in a time domain analysis is not periodic with constant amplitude, the equation of motion in frequency domain (Eq. (9)) cannot be directly converted to following form of the time domain as the added mass and radiation damping are frequency dependent (ANSYS, 2013);

$$(M_s + M_a)\ddot{X}(t) + C\dot{X}(t) + KX(t) = F(t) \quad (14)$$

Instead, the equation of motion can be written in convolution integral form;

$$(M_s + A_\infty)\ddot{X}(t) + C\dot{X}(t) + KX(t) + \int_0^t R(t-\tau)\dot{X}(\tau)d\tau = F(t) \quad (15)$$

Here, M_s is the structural mass matrix, A_∞ is the fluid added mass matrix at infinite frequency, C is the damping matrix, K is the total stiffness matrix and R is the velocity impulse function matrix.

4 STATE OF THE ART REVIEW OF AC/DC & PLATFORM WINDFARM CABLING

To get in depth detailed knowledge about wind farm and cabling arrangement, a thorough literature study is carried out in the presence of previous works by different authors and standards. Also, details of electrical cables and cable connections to a floating substation from wind turbines in deep water case are described in this section of the report.

4.1 Typical Offshore Wind Farm Arrangement

A typical offshore wind farm arrangement from wind to onshore grid is shown in the Figure 2.

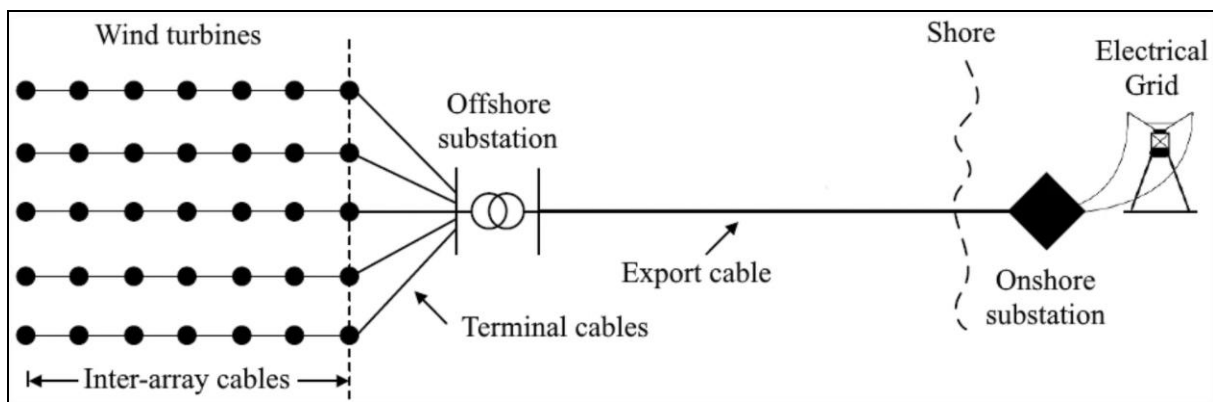


Figure 2: A typical offshore wind farm energy transport diagram (W.-S.Moon, 2014)

From a series of the wind turbine, the electricity will be collected in offshore substation such as GICON AC/DC TLP substation. Low voltage electricity converts to high voltage electricity in substation platform to reduce the transmission loss while transferring long distance from offshore substation to onshore substation. From onshore substation, the electricity can transfer to the onshore electricity grid.

4.2 Electric Cable

A typical 3-phase AC subsea power cable cross section is shown in Figure 3.

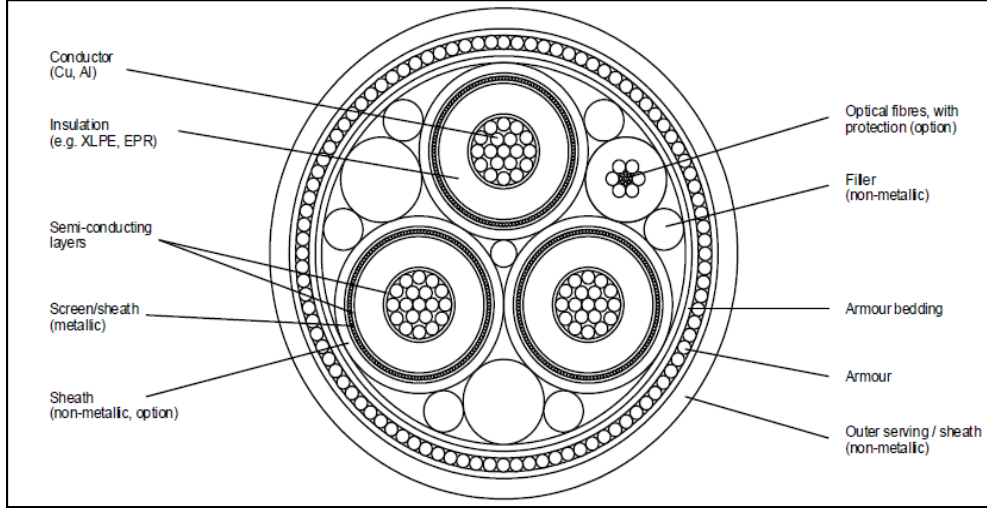


Figure 3: Typical 3-Phase AC subsea power cable cross section (DNVGL-ST-0359, June, 2016)

A cable is an assembly consisting of one or more power cores with individual or common screen and sheath, assembly fillings and covered by a common protection (DNVGL-ST-0359, June, 2016). Also, the cable can contain optical fibers for communication and cable monitoring purposes. The cable type and properties have to be selected by considering the generator capacity and on shore grid voltage for connection (TANINOKI, 2017). Cables are subjected to main dynamic load in lateral direction mainly due to the motion of the floating structure and there has been high probability to damage the insulation of the cable. Also, another point of maximum stress is at the bottom/sea bed due to the repetitive wear at the contact of seabed. In cables, main strength/stiffness are provided by the armour which can have double or triple layers (TANINOKI, 2017). And the selected cables should meet the criteria given by International Electrotechnical Commission (IEC) standards and DNVGL-ST-0359 rule. The armour coil different type of layups is shown in the Figure 4.

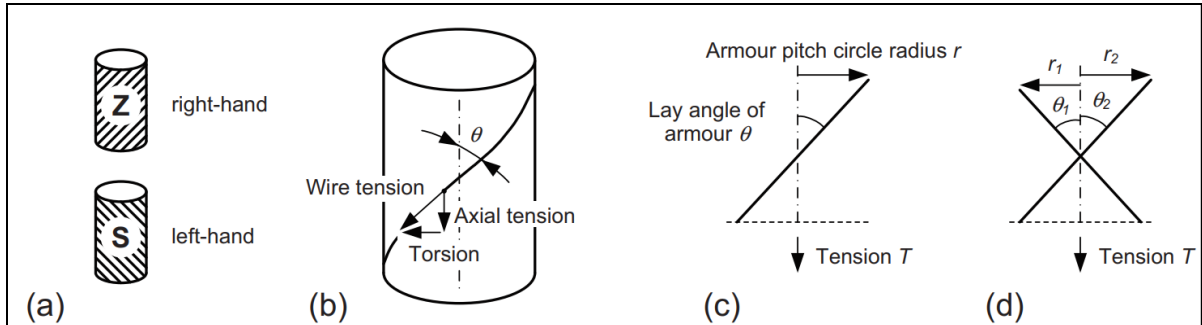


Figure 4: Cable armour. (a) Z- and S- lay, (b) forces, (c) unbalanced armour, (d) torsion balanced armour (DNV-RP-J301, 2016)

4.3 Factors Influencing the Design of Optimal Cable Path

The arrangement of electrical cable connection to a floating platform will depend on the various factors. The cable lines and accessories have to be designed in accordance with the environmental condition in the installed location. The mechanical strength requirement that is to be taken care while designing the cable arrangement to floating substation are described as follows;

- Stress generated in the cable and cable components (mainly at the location of cable entry to supporting structure)
- Minimum Bending Radius (MBR) of cable
- Minimum distance between cable to cable/ cable to mooring/ cable to structure under external dynamic loading to avoid collision.
- Minimum distance of the cable over hangs (in case lazy wave shape arrangement) to water line and seabed.
- Fatigue life of the cable
- Tearing and wearing of cables
- Temperature dependency of strength properties.

As the substation is floating TLP in deep sea, the offset distance in surge and sway will be large compared to heave motion. So, the cable arrangement or connection should adapt these distances without crossing the design criteria. With respecting the required criteria, different possible global arrangements of the cable layout to TLP substation are shown Figure 5 and Figure 6.

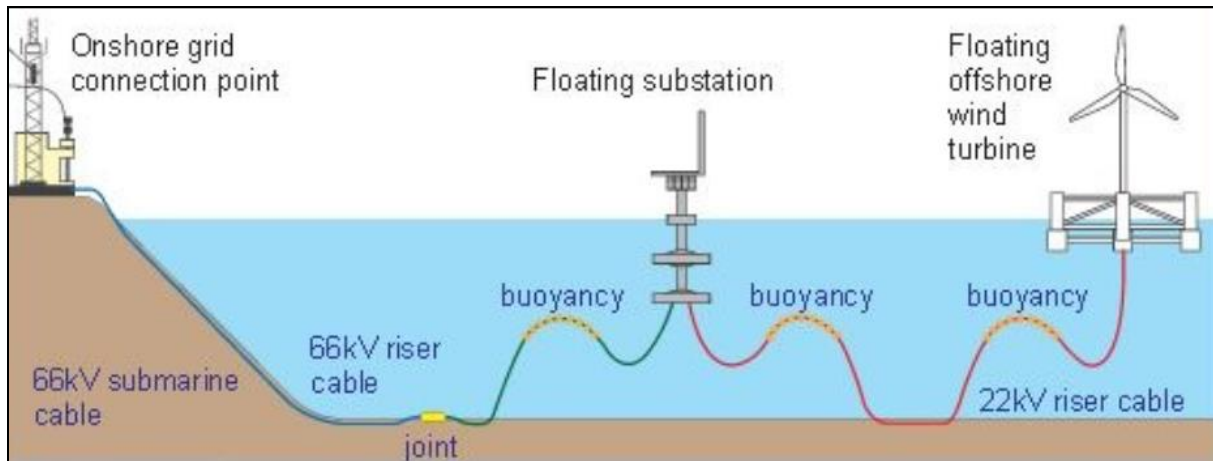


Figure 5: Cable connection between wind turbine and substation – lazy wave shape

(<https://w3.windfair.net/wind-energy/news/17254-inside-offshore-wind-fukushima-floating-offshore-wind-farm-demonstration-project>)

To avoid large motion of cables the offset can be restricted by using strings/wire which can be connect the cable to seabed as shown in Figure 6.

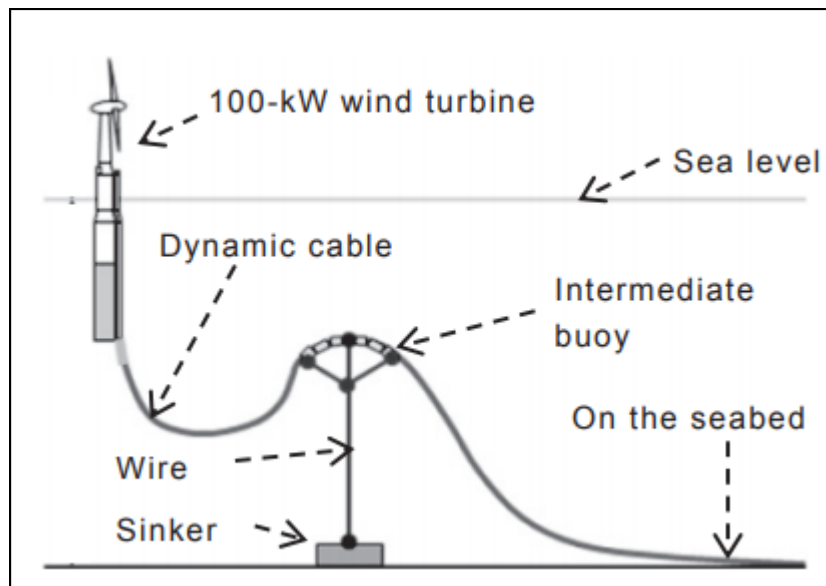


Figure 6: Cable connection on floating structure – lazy wave with wire (TANINOKI, 2017)

The wire and sink arrangement shown in the Figure 6 will help to maintain the minimum bending radius or kinking along the cable length and avoid the collisions. The main disadvantage of the above arrangement is the over restriction of the electrical cable due to the arrangement of the wire (as taut) which may cause higher stress on the cable. To avoid this,

usage catenary wire instead of taut wire will help to restrict the motion of the cable without having large stress in the cable.

Double lazy wave shape by additional buoyancy elements on the electrical cable can also reduce the cable tension.

4.4 Components in Cable Lay-outing

4.4.1 Cable buoy

Due to the environmental loads acting on the floating structures, an adequate loose length of the cables is required to limit the criteria of minimum bending radius and maximum tension on the cable. This can be achieved by the cable buoys which will be fixed on the electrical cable and give additional buoyancy for the cable and adapt to required shape and length. A typical arrangement of the cable buoy on the floating structure are shown in Figure 7.

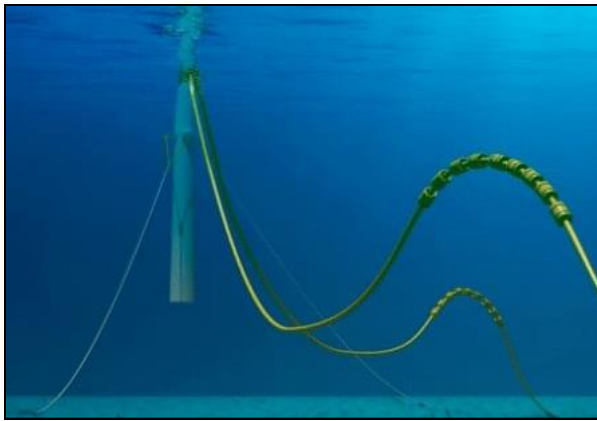


Figure 7: Cable buoy

(<https://www.ablison.com/offshore-wind-farm-facts/>)

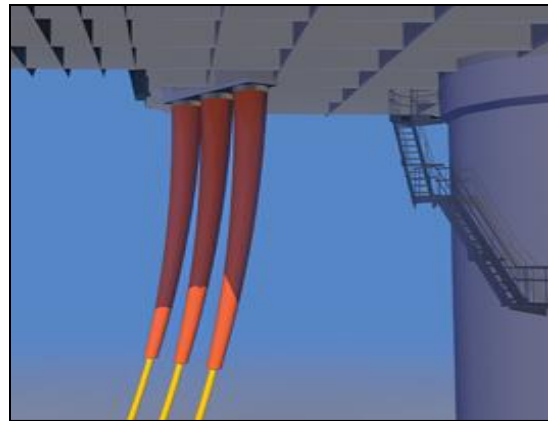


Figure 8: Bend stiffeners

(<https://petrolcomuae.com/wp-content/uploads/2019/04/bend-stiffeners.jpg>)

The distance between the buoy and location of the buoy can be chosen to reduce the tension and radius greater than minimum bending radius of the cable in all the condition.

4.4.2 Dynamic Cable Bending Stiffeners

One of the main locations of the cable failure is at the connection of the cable with floating structures. The lesser stiffness cable is connected to high rigid bottom structure which moves drastically causes large stress spot in cable at connection points. This stress can be reduced by using bend stiffener at the connection point.

Bending stiffeners have large stiffness compared to the cable to take larger loads at the connection points. The stiffness of the bend stiffeners will be higher at the connection point and gradually reduced over a length by tapering the cross section as shown in the Figure 8.

4.4.3 Cable Bending Resistor

To avoid excessive bending/kinking of the electrical cables, bending resistor can be installed on the cable. Bending stiffeners will take the bending stress after a particular bending moment and reduce the harm on the cables. Figure 9 and Figure 10 shows the detail of the bending resistor.

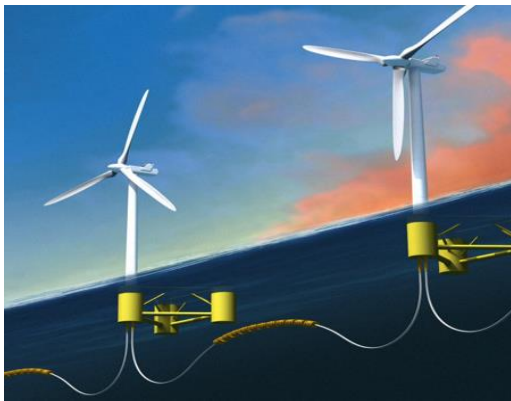


Figure 9: Cable bending resistor (*)

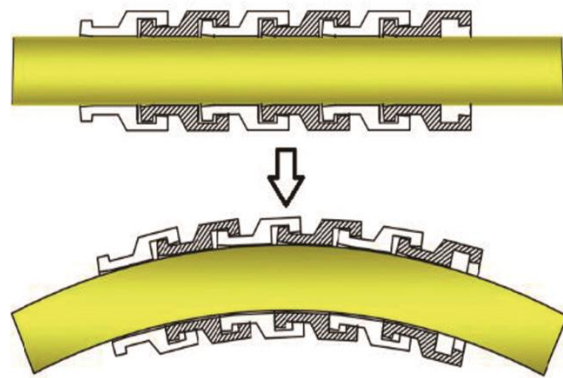


Figure 10: Elevated section view of cable bending resistor (**)

*Courtesy:<https://www.balmoraloffshore.com/images/products/offshore-wind/floating-offshore-wind-turbine-2.jpg>

**Courtesy:<https://www.energychina.press/fileNFNYJS/journal/article/nfnyjs/2020/2/PIC/eb9020d5-65fd-46cf-9286-506420813140F008.png>

4.4.4 J or I tube

J and I tubes are open ended pipe attached to the floating structures which will guide the electrical cables to specific direction and protect at the connection to floater. Figure 11 shows a typical I tube.

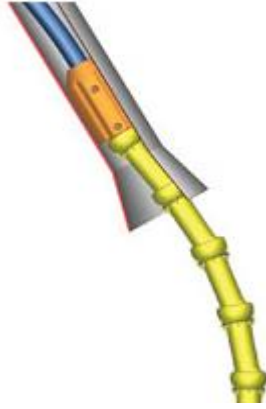


Figure 11: “I”-tube section

(Blue Ocean - Cable Protection Products (blueoceanprojects.com))

As shown in Figure 11, At the end of the tube, to reduce the wear and tear on the cable a bell mouth is fitted. The cables can be routed inside the floating units through fixed tube (J/I tube) or flexible tube (tube less). The design requirement of the tubes as per the DNV-RP-J301 (DNV-RP-J301, 2016) are pointed out below,

- Tubes shall be sufficiently sized, shaped and have a smooth inner surface to allow passage of the pulling device, cable end and cable without exceeding cable integrity limits.
- When mounted externally to a structure, the tube shall be able to withstand impact forces specified in the design basis.
- Tubes should be made of steel or, alternatively, of material type tested for the application.
- The inner diameter of J-tube should not be less than 2.5 times the cable outer diameter to facilitate cooling and to avoid excessive pull in force.
- The bending radius of the J-tube should not be less than $20 \times$ cable outer diameter in order to facilitate the cable installation.

4.4.5 Burial and Non-burial of Cables at Sea bed

At sea bed, to protect the cables from external loading, burial and non-burial techniques can be used. The main type of burial methods are shown in Figure 12.

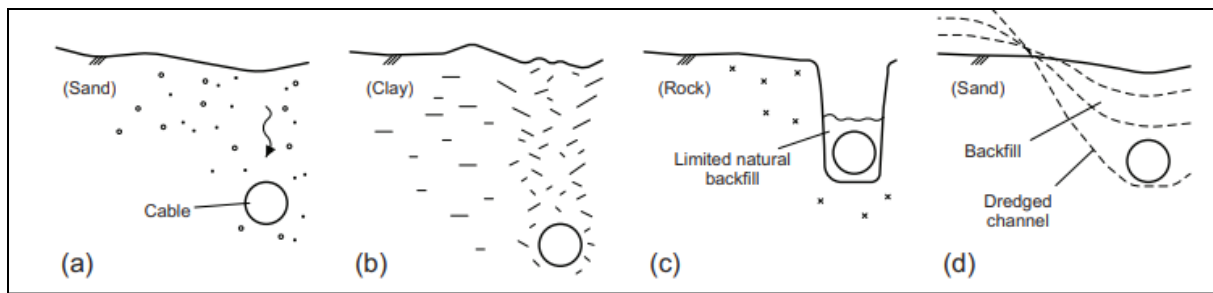


Figure 12: Various burial condition of cable at sea bed (DNV-RP-J301, 2016)

The non-burial methods are done by using the help of split pipe section, block section interconnected by rope loop or covering the cable with stones as shown in Figure 13.

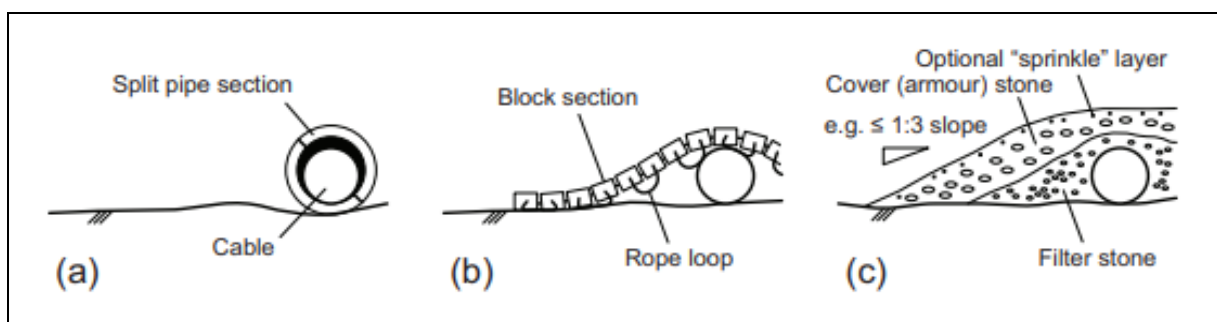


Figure 13: Various non-burial condition of cable at sea bed (DNV-RP-J301, 2016)

4.4.6 Cable Hang-offs

The hang-off should be capable of to securely hang the cables on floating structures by transferring the loads from armour to structure without compromising the integrity of the cable (DNV-RP-J301, 2016). As shown in the Figure 14, there mainly two parts for the hang off – frictional based and permanent hang off. A compression load will apply to the frictional based hang off to hold the cable. In permanent hang off, the armour wire will be used to hold tight.

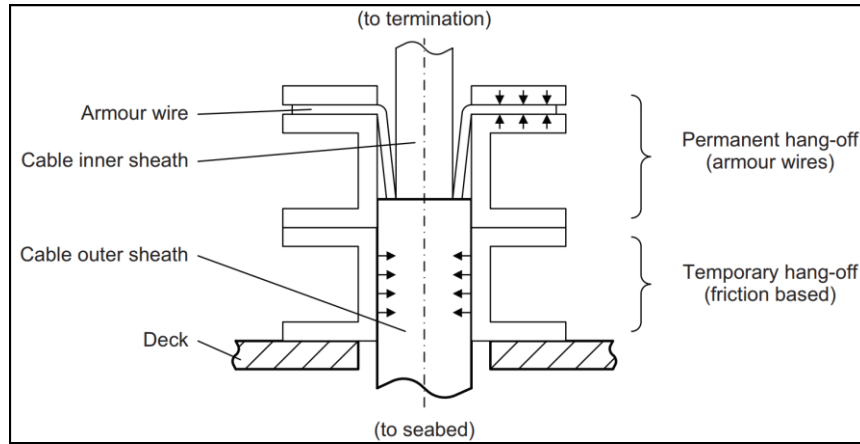


Figure 14: Typical design of the cable hang-off (DNV-RP-C205, 2010)

The hang-off should also provide watertight integrity for the arrangement.

4.4.7 State-of-art-review for Hydrodynamic Analysis of TLP platforms

The hydrodynamic analysis of TLP platforms are quite well studied in past decades by many authors. A thorough literature study is carried out in order to analyze the previous works by different authors.

A comparison study of TLP, semi-submersible and Spar platforms are done in hydrodynamic aspects by Binbin Li et al (Binbin, 2011). The paper compares the global motion characteristics of the platforms using 3D potential theory. The analysis results show that, the pitch and heave responses of the TLP platforms are small compared to other platforms. But the surge response of TLP is greater compared to other platforms due to its weak surge stiffness. Also, the Low Frequency motion of surge becomes more dominating than the Wave Frequency motions with a decrease of the peak period of wave spectrum.

Rentschler et al (Rentschler, et al., 2020) give an insight to hydrodynamic pre-design of dynamic cables (electrical cables). Numerical analyses are compared for the dynamic cables shapes -catenary and Lazy wave shape. A parametric study has been carried out to find the optimal length of the cable for each shape in given water depth. The paper concluded that the lazy wave shape is technically superior to the catenary shape in hydrostatic aspects. The results based on hydrodynamic analysis were out of scope of the paper.

Shilun Zhao et al (Zhao, et al., 2021) have done a comparison of lazy wave and double lazy wave configuration on TLPWT in shallow water. For the study both hydrostatic and

hydrodynamic aspects were compared. The result showed the double wave offered the superior performance compared to lazy wave.

Erin E. Bachynski et al (Bachynski & Moan, 2012) describes the design consideration of Tension Leg Platform Wind Turbines (TLPWT). Some of the design considerations listed can be applicable to ordinary TLP platforms also. Careful choice of natural period, diameter at the water line, ballast, pretension, and pontoon radius can be used to improve the TLPWT performance in different environmental conditions and water depths.

A numerical procedure for the prediction motion response of the tension Leg Platform in waves are described by Chuel-Hyun Kim et al (Kim, et al., 2007). The developed TLP platform is assumed to be flexible in lieu of rigid to capture more accurate results. The numerical approach is by considering the coupling analysis using Finite Element method (FEM) and potential solver. So, both hydrodynamic response and structural response are considered to be linked simultaneously in this analysis approach. The hydro-elastic method are applied to the radiated force due to the elastic nature of the superstructure of the TLP platform.

4.4.7.1 Comparison of cabling arrangement in different type of floating platforms

Due to the design constraints of electrical cables on floating structures, the cabling arrangement will be different due to their mooring arrangement and other parameters such as hydrodynamic characteristics of the platforms. Here, the cabling layout for three main floating substations (Semi-submersible, TLP and Spar platforms) are compared.

To have the support for the cables, the connection of the cable to substructure is arranged near to the pillars.

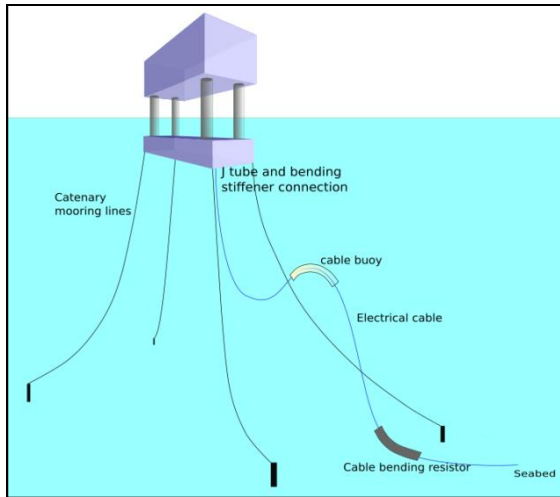


Figure 15: Semi-Submersible Platform mooring and cabling arrangement

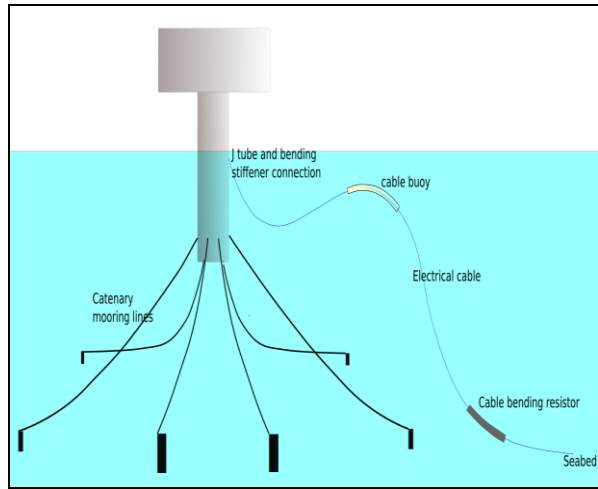


Figure 16: Spar Platform mooring and cabling arrangement

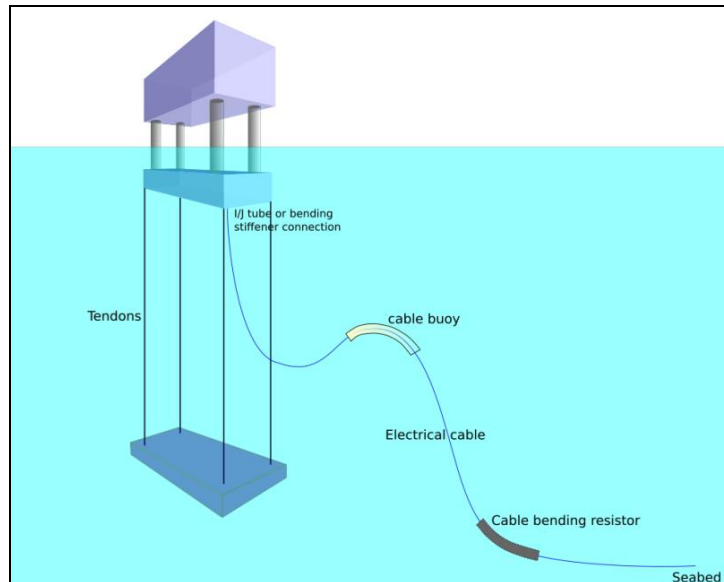


Figure 17: TLP mooring and cabling arrangement

For Semi-submersible and Spar platforms, as the mooring lines are loosely connected to the seabed, the probability of collision between the electrical cables and mooring lines are higher than TLP structure because TLP has almost straight mooring lines to seabed. Moreover, for Semi-submersible and Spar platforms, the part of electrical cable nearest to the substructure is more critical compared to TLP due to the large motion characteristics of the Spar and Semi-submersible compared to TLP. For TLP substructures, due to less pitch and heave motions, the cabling arrangement and design (less stress due to low bending of the cable at connection helps for longer life) will be easier compare to other floating substructures.

5 METHODOLOGY AND RESULTS FOR HYDRODYNAMIC ANALYSIS OF TLP

The entire hydrodynamic analysis is carried out using ANSYS potential theory solver, ANSYS Aqwa. ANSYS Aqwa can be used to find the response of any moored/unmoored floating structures for a given set of environmental loads using potential theory. In this part of the report, the steps involved in the analysis of AC/DC TLP platform are described in detail. Figure 18 shows a flow chart describes the steps involved in the analysis,

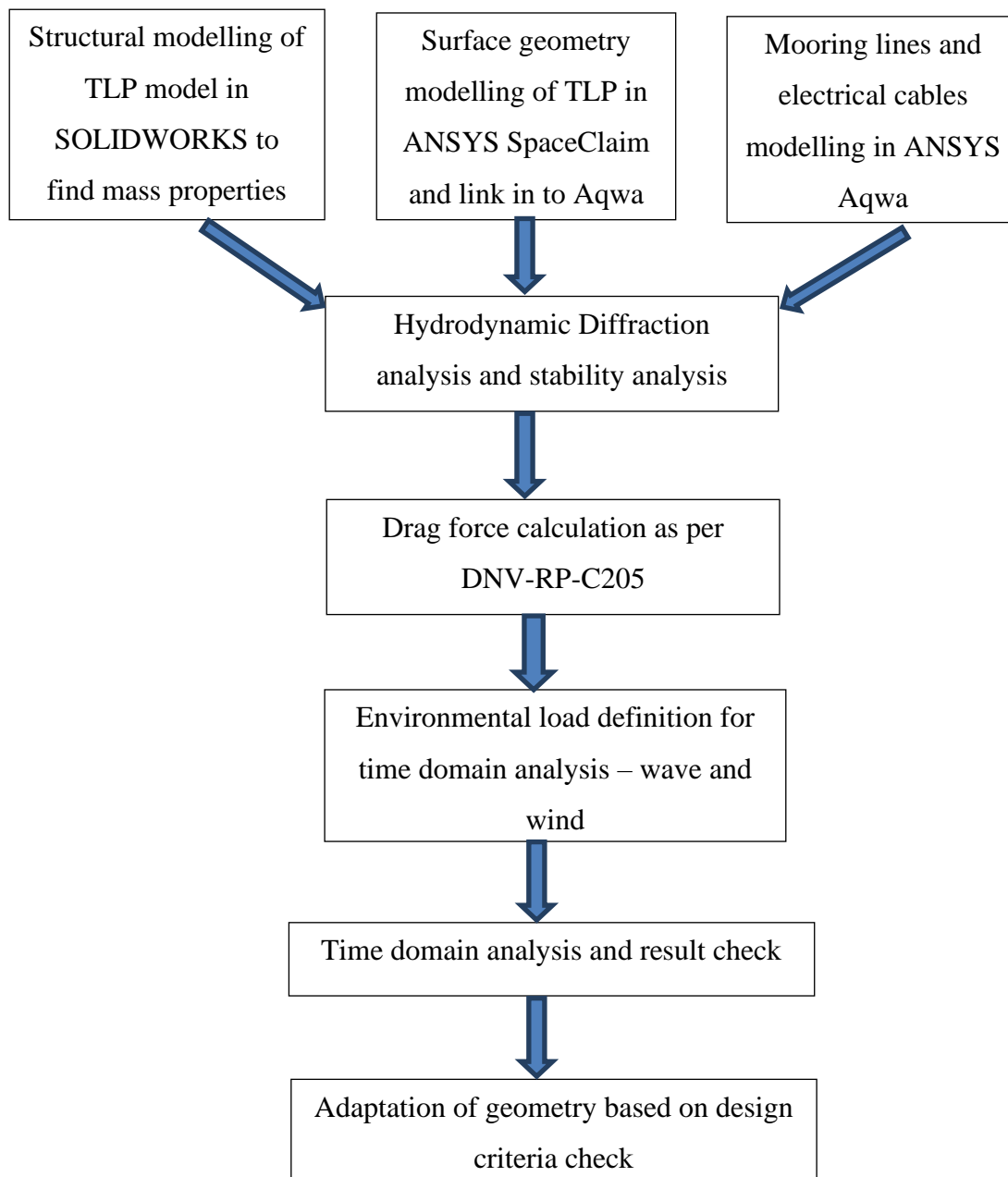


Figure 18: Steps used for hydrodynamic analysis of TLP

5.1 Co-ordinate System Used in ANSYS Aqwa

The direction of the waves/wind about the structure are shown in Figure 19.

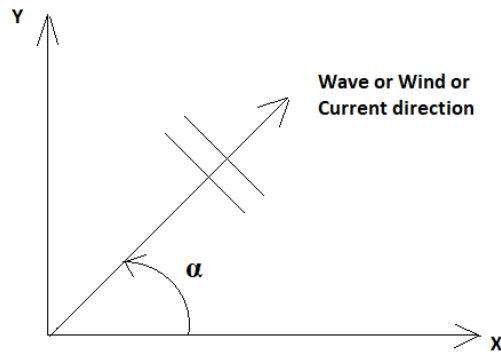


Figure 19: Direction of Wave/Wind/current

Here, α is the angle between global x-axis and wave/wind/current direction.

5.2 Environment Loads

The hydrodynamic analysis is developing for the potential implementation of the GICON AC/DC TLP platform near North Atlantic Sea. The wave and wind data corresponding to specified location are used. The load data set is then extrapolated to 100-year return period – Ultimate Limit State (ULS). Mainly two load cases for ULS are considered – Regular and Irregular wave case.

5.2.1 Regular Wave, Wind and Current – Regular Wave ULS

Regular wave with 100-year return period is used for the simulation. The wave height and period considered for the analysis is,

Maximum wave height, H_{max} : 25.26m

Wave period, T : 13.89 sec

The 100-year return period wind speed at reference height (10m above water line) = 33 m/s is used for the analysis. As per the data in the location, the current velocity considered as zero.

5.2.2 Irregular Wave, Wind and Current - Irregular Wave ULS

Irregular wave with 100-year return period for the simulation are,

Significant wave height, H_s : 13.54m

Zero crossing period, T_z : 10.8 sec

Spectrum used : JONSWAP spectrum (with average value of

$\gamma=3.3$). As the location of the site is near to North Atlantic Sea, JONSWAP spectrum is the best fit spectrum. As per DNV-RP-C205 (DNV-RP-C205, 2010), Peak period, $T_p = 1.2859 * T_z = 13.89$ sec for the given spectrum. The 100-year return period wind speed at reference height (10m above water line) = 33 m/s is used for the analysis. As per the data in the location, the current velocity considered as zero.

5.3 Mass Properties of Platform

Mass, center of gravity and mass moment of inertia about the center of gravity has to calculate accurately to analyze the hydrodynamic response of the platform. The entire model and equipments weight have been modeled in SolidWorks to retrieve the mass properties of the full model.

As the objective of the work is to convert the existing GICON O&M TLP platform to AC/DC TLP platform, the main dimensions of O&M TLP platforms are replicated to AC/DC TLP platform. But the top side structure depth is increased for AC/DC TLP platform (without modifying the depth of vertical column) due to addition of the cable deck for easy storage/operation of the electrical cables and presence of large height equipments. The weight estimation details cannot be shown due to the confidentiality of the report.

5.4 Hydrodynamic Modeling of Geometry

To calculate the hydrodynamic loads by waves on the structure, the structure should be modeled either by assuming large volume structure (2D elements) or small volume structure (Morison elements). The term large volume will be used if the geometrical size, D is same order of magnitude as that of wave length, λ . usually, $D > \lambda/6$. Large volume structure will be inertia dominated and small volume structure will be drag dominated. The rule (DNV-RP-C205, 2010) depicts the prevailing nature of different forces on the structure through the Figure 20.

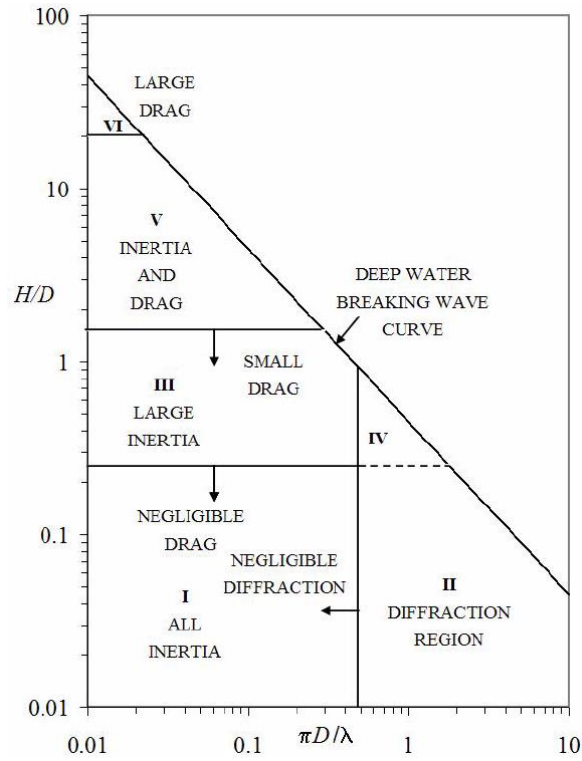


Figure 20: Different wave force regimes (DNV-RP-C205, 2010) (H: Wave height, D: characteristic dimension)

A linear analysis will usually be sufficiently accurate for global wave frequency loads (DNV-RP-C205, 2010). This means, for irregular wave, the response of the structure can find by superimposing the individual wave responses. The calculations cannot be shown in the report due to confidentiality.

$$\text{Wave height, } H = 2 \cdot \sqrt{(2 \cdot S(\omega) \cdot d\omega)} \quad (16)$$

$$\text{Wave length, } \lambda = (g \cdot 2\pi) / \omega^2 \quad (\text{dispersion relation for deep water case}) \quad (17)$$

$S(\omega)$: Spectral Ordinate ($\text{m}^2/(\text{rad}/\text{sec})$)

$d\omega$: difference between consecutive frequency in **Error! Reference source not found.** ($=0.03 \text{ rad}/\text{sec}$)

ω : Wave frequency (rad/sec)

D : Characteristic dimension of the column ($=5.7\text{m}$) and pontoon (9.0m)

g : $9.81 \text{ m}/\text{s}^2$

From the calculation, It is clear that both column and pontoon of TLP platform are in inertia dominated region in the graph shown in the Figure 20 (Region I and III). The surface of the structure can be modeled by using 2D elements which will help to calculate diffraction force

and radiation force. As the solver is based on potential theory, to include the viscous drag force due to waves/current, dummy Morison elements are modeled inside the structure (due to confidentiality of the work, the ANSYS model has not shown in the report). To avoid the addition of inertial load twice, the added mass coefficient for dummy Morison element is input as zero (which is already calculated by 2D elements/panels). To add viscous drag-only force on the members, the actual cross-section area of the members scaled down by 100 and actual drag coefficients of the structures scaled up by 100 (by which the inertia component can be neglect). This can be explained by following Morison equation,

$$\text{Morison force, } F = \frac{1}{2} \rho D C_d (u_f - u_s) |u_f - u_s| + \rho A C_m \dot{u}_f (\approx 0) - \rho A C_a \dot{u}_s (\approx 0) \quad (18)$$

Here, density of water, ρ : 1025 kg/m³

Drag coefficient, C_d : Calculated as shown in the section 5.8.1 (=100 times C_D)

D : $\frac{\text{Characteristic dimension of structure (in m)}}{100}$

u_f, \dot{u}_f : Fluid particle velocity and acceleration normal to line body respectively

u_s, \dot{u}_s : Structural velocity and acceleration normal to line body respectively

Added mass, C_a : 0

Inertia coefficient, C_m : $1 + C_a$

Due to scaling down of the structural dimension and scaling up of drag coefficient, 2nd and 3rd terms of the equation can be neglect and only 1st term of the equation will have the significant value which is viscous drag force.

The geometry split at waterline (=22m above base line) to make sure that the elements (diffracting and non-diffracting elements) are not created on the water line and ensured the continuity of the elements at waterline using “merge” tool in SpaceClaim. The elements below the water line will be diffracting elements and above will be non-diffracting elements. Also, the normal of the surface should be outward.

The Boundary Element Method (BEM) is a numerical approach which assumes constant source/sink strength over a mesh. To validate the mesh size, a convergence study or mesh independence study need to be assessed. The objective of this study is to get required mesh

size for the accurate hydrodynamic response analysis with less computation time. Also, the mesh size depends on the frequency range for the analysis. It means, for large mesh size only limited frequency range can be used for the analysis. So, it is required to select smallest mesh size which give accurate hydrodynamic response with better geometric approximation and less computation time. Moreover, in ANSYS Aqwa, the maximum number of elements is limited to 40,000 which will be achieved for the maximum mesh size of 0.8 m. The added mass and radiation damping coefficient of the structure for the range of wave frequencies were compared for different mesh size.

The hydrodynamic coefficients are almost equal for different mesh sizes. For better geometric approximation, the mesh size of 1.5mx1.5m is used for further analysis.

5.5 Hydrodynamic Diffraction (HD) Analysis

The Hydrodynamic Diffraction (HD) analysis provides first & second order forces and its response (Response Amplitude Operator (RAOs) and Quadratic Transfer Functions (QTF)) of the floating body without the effect of the mooring lines and drag forces (but the drag force can be included in the analysis by linearizing the drag forces) in frequency domain.

In HD analysis, a range of frequencies are considered which includes the typical natural periods of motion of TLP platforms and wave frequencies. The range of frequency and wave direction considered for the analysis as follows,

Longest frequency : 0.0628 rad/sec (Time period, $T = 100$ sec)

Shortest frequency : 2.792 rad/sec (Time period, $T = 2.249$ sec)

Frequency step : 0.113 rad/sec

No. of frequency : 25

Direction of the waves: 20-degree wave interval (17 waves)

The hydrostatic solution, RAOs and QTFs are the solutions after HD response analysis. From hydrostatic solution, hydrostatic parameters can be found for the given waterline split of TLP platform. The displacement of the floating structure for the given waterline can be used to find the pretension in the mooring cables.

5.6 Mooring Lines Properties

The mooring lines of the TLP platform are called tendons/tethers. These are high strength steel cables under high pretension to arrest the motion of the platform. The material properties of the tether cables used for the initial analysis are tabulated below,

Table 1: Tendon's properties

Properties	Values
Young's Modulus, E (N/m ²)	2.06E+11
Diameter of cable, d (m)	0.3
Area of cross-section, A (m ²)	0.0706
Total number of cables	one at each corner (total 4 Cables)
Maximum stress (N/mm ²)	235

The end coordinates of the tendon connection on platform and sea bed are shown in Table 2.

Table 2: Co-ordinate of mooring end points

Co-ordinate of cable connection	X_Co-ordinate (m)	Y_Co-ordinate (m)	Z_Co-ordinate (m)
CP 1	20	20	-15
CP2	-20	20	-15
CP 3	-20	-20	-15
CP 4	20	-20	-15
FP 1	20	20	-200
FP 2	-20	20	-200
FP 3	-20	-20	-200
FP 4	20	-20	-200

Note: CP is connection point on the structure which is free to move with the structure and FP is fixed point which will be always fixed. The tendons will connect between CP1&FP1, CP2&FP2, CP3&FP3, CP4&FP4.

5.6.1 Calculation of Pretension & Unstretched length of the Tendons

Pretension is the tension on each tendon which holds the TLP platform in still water static position. It will depend on the difference between buoyancy and weight of the structure. The unstretched length of the tendon is the length of the mooring line at still water condition.

For preliminary analysis, the Water Line position is located at 22m above base line. From the detailed calculations (calculation is not shown due to confidentiality reason), the pretension on one cable at still water condition = $F/4 \times 9.81 = 10571335.71$ N.

5.7 Stability Analysis

Stability analysis is the first step of the dynamic analysis to find the starting position or equilibrium position of the floating structure. An iterative approach is done by Aqwa to find the equilibrium position of the structure. At each step, software calculated the hydrostatic forces and moments over all wetted elements corresponding to moored condition of the structure.

In stability analysis, Aqwa gives different modes of motion, its natural period and damping ratio relative to critical damping (%) for moored TLP platform. The values are tabulated as shown below,

Table 3: Natural period and damping ratio

Motion modes	Natural period, T_R (sec)	(%) of critical damping
Surge	45.21	0.28
Sway	45.20	0.31
Heave	1.27	0.00034
Roll	0.92	0.026
Pitch	0.92	0.026
Yaw	18.86	0.17

(Note: % of critical damping, $\xi_c = -\frac{C}{2\sqrt{MK}} \times 100$ %; where, C, M and K are damping coefficient, Mass of structure and stiffness of the motion respectively).

From the result, it is clear that heave, pitch and roll motion have the very small natural period as expected due to the presence of large restoring force by tendon stiffness.

Even though, the wave frequencies are outside the range of natural period of the TLPs, the second order force due to interaction of the different waves can excite at natural period which can cause resonance of the motion.

5.8 Hydrodynamic Response (HR) Analysis

Time domain analysis is used to find the response of the structure for ULS condition. In normal operation environmental conditions perturbation approach can be used to find the response of the structure under the assumption of small wave steepness and response of the floating structure. But for severe wave conditions such as ULS, perturbation approach will not be valid because of high wave amplitude and structural response. For this reason, a special tool called ANSYS Aqwa-Naut is used to find the response for both regular and irregular waves ULS cases. This calculation is performed at each time step of the simulation, along with the instantaneous values of all other forces (ANSYS, 2013). These forces are then applied to structures, via a mathematical model and the resulting accelerations are determined. The position and velocity at the subsequent time step are found by integrating these accelerations in the time domain, using a two-stage predictor-corrector numerical integration scheme (ANSYS, 2013).

Motion damping forces of floating structures are due to radiation damping force, hull skin friction damping, hull eddy making damping etc. The radiation damping will be taken care by potential theory, but viscous effect has to be input manually. The drag coefficient (C_D) is usually calculated by simplified formulas or from experiment or from Computational Fluid Dynamics (CFD). In this report, viscous drag is calculated by analytical equations explained by the rule (DNV-RP-C205, 2010).

5.8.1 Current Drag Coefficient Calculation

There are two types of underwater structural elements for the AC/DC TLP platform – vertical cylindrical column and horizontal pontoon rectangular structure. The C_D value will depend on the Reynolds number (Re), Keulegan-Carpenter number (Kc) and roughness of the surface. For cylindrical cross-section structure, the variation of C_D at different Re, Kc and roughness

are available in the rule (DNV-RP-C205, 2010). But for rectangular cross-section, only drag coefficient independent of these parameters is available.

5.8.1.1 For Cylindrical Cross-section

An iterative approach has to be followed to include the velocity of the structure in the equation of Re and Kc. In first iteration, the velocity of the structure is an unknown and Re, Kc and C_D has to calculate by considering only the velocity of the flow (using 1st order stokes equation). In the next iteration step, relative velocity between the structure (from the software ANSYS Aqwa using previous input) and fluid particle velocity (using 1st order stokes equation) can be included in the calculation of Re and Kc and it will help to find the exact value of C_D . This will lead to retrieve the response of the structure with reasonable accuracy.

$$\text{Reynolds number, } Re = uD/\nu \quad (19)$$

$$\text{Keulegan Carpenter number, } Kc = uT/D \quad (20)$$

Where, u : Maximum relative velocity between structure and flow (m/s)

D : Characteristic dimension of the structure (m)

ν : Kinematic viscosity of the sea water ($= 1.19\text{E-}6 \text{ m}^2/\text{s}$)

T : time period of the wave (sec)

To calculate the Re and Kc in irregular sea, significant fluid velocity (velocity corresponding to the significant wave height) has to be considered as per DNV -RP-C205 (DNV-RP-C205, 2010). The significant fluid velocity at “z” meter below water line can be approximated by using 1st order stokes equation in deep water condition,

$$V_s(z) = \frac{\pi H_s}{T_p} e^{k_p z} \quad (21)$$

Where, k_p : Wave number corresponding to a wave period, $T_p (= \frac{2\pi}{\lambda})$

z : vertical co-ordinates (m), positive upward where mean surface is at $z=0$.

λ : Wave length (m)

5.8.1.1.1 First Iteration to Find C_D

As the structural velocity is unknown initially, the Kc and Re can calculate by only considering the velocity of the flow.

a) Effect of Reynolds number (Re) and roughness (k)

Two-dimensional drag coefficients for circular cylindrical section for different roughness value are well defined in literatures as shown in the Figure 21.

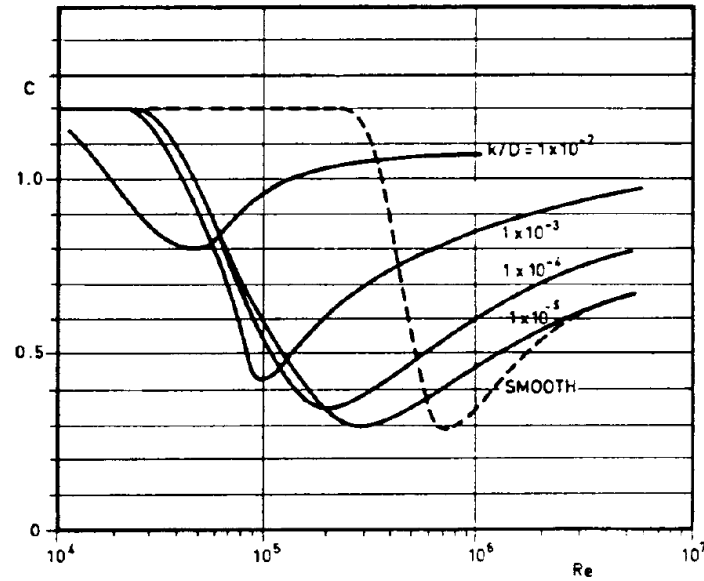


Figure 21: Drag coefficient for circular cylindrical section for various Re and roughness (k), (DNV-RP-C205, 2010)

It is clear from the figure that, there is large drop in drag coefficient for circular cylindrical section on intermediate Re value. This area is called critical flow regime. But for ULS case, more often the cylinder will be in post critical flow regime and drag coefficient will be constant.

By using 1st order stokes equation Eq.(21), for ULS wave condition ($H_s=13.54\text{m}$, $T_p=13.89\text{m}$), the horizontal velocity of the fluid particle at $z=10\text{m}$ is 2.48 m/s . This flow velocity has Re equal to $1.19\text{E}+7$. Moreover, to have more conservative response of the structure, roughness of the structure is considered as “smooth” for which $k = 5 \times 10^{-6}$ as per DNV rule (DNV-RP-C205, 2010). From Figure 21, for the calculated Re and roughness value, the value of drag coefficient (C_{DS}) of the vertical column can be approximated as 0.65.

b) Effect of keulegan-Carpenter number (Kc)

The value of C_{DS} calculated for the Re has to be multiplied by a correction factor, called wake amplification factors (Kc). The variation of (Kc) over Kc/C_{DS} are shown in the Figure 22.

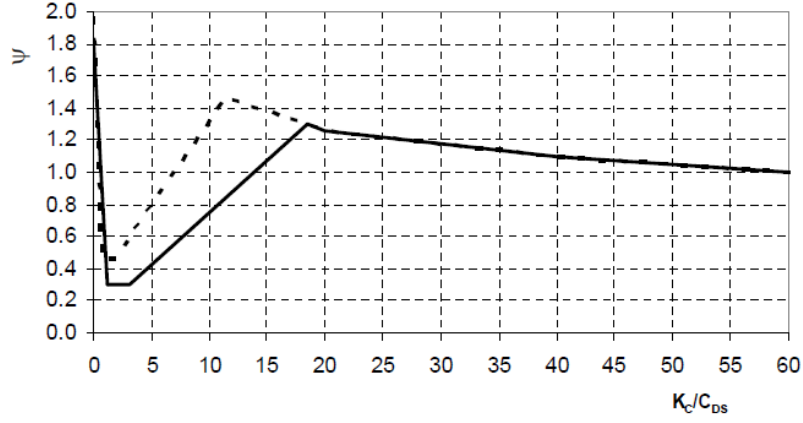


Figure 22: Wake amplification factor as function of Kc number for smooth (solid line- $C_{DS} = 0.65$) and rough (dotted line- $C_{DS} = 1.05$) (DNV-RP-C205, 2010)

Using the Eq. (20), the value of Kc for the velocity 2.48 m/s will be 6.05 and the ratio Kc/C_{DS} equal to 9.31. From the Figure 22, the wake amplification factor will be 0.702.

So, the drag coefficient, $C_D = C_{DS} * \Psi(Kc) = 0.65 * 0.702 = 0.457$

5.8.1.1.2 Second Iteration to Find C_D

To find the exact drag coefficient (C_D) of cylinder, the maximum relative velocity between structure and flow has to be considered in the equation of Re and Kc. By using C_D value from section 5.8.1.1.1 and 5.8.1.2, the horizontal velocity of the structure for ULS condition can be found using time domain analysis. The maximum horizontal velocity of the structure is found to be 2.5 m/sec. The maximum relative velocity of the structure will be the sum of fluid velocity (2.48m/s) and structural velocity (2.5 m/s), which is equal to 4.98 m/s.

a) Effect of Reynolds number (Re) and roughness

Even though, Re has been increased compared to the first iteration due to the consideration of structural velocity, the coefficient C_{DS} will be same as the initial value ($=0.65$) because of the constant value of the drag after critical flow regime shown in the Figure 21.

b) Effect of Keulegan Carpenter number (Kc)

The Kc value increased due to increase in velocity which will be equal to 12.14. The wave correction factor from Figure 22 will be equal to 0.9 and the final drag coefficient will be,

So, the drag coefficient, $C_D = C_{DS} * \Psi(Kc) = 0.65 * 0.9 = 0.585$

This value has been used as drag coefficient of the cylindrical column for the entire response calculation.

5.8.1.2 For Pontoon- Rectangular Cross-section

For the rectangular horizontal structures (pontoon structures), as per DNV rule (DNV-RP-C205, 2010) the value of the drag coefficient is independent of the Re, Kc and roughness. And it depends only on the cross-sectional dimension of the structure.

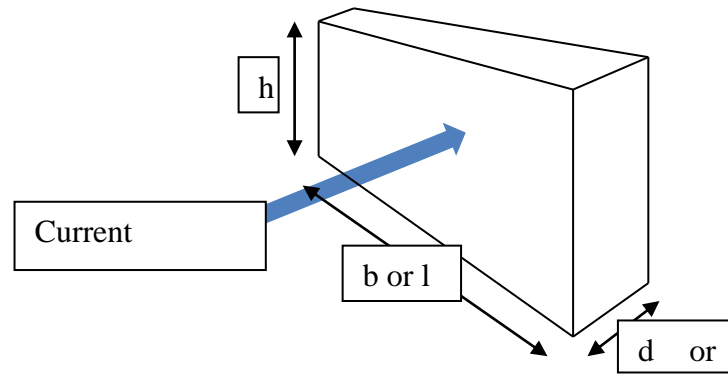


Figure 23: Orientation of rectangular cross section against the current

The drag coefficient of rectangular cross section is shown in the Table 4,

Table 4: Drag coefficient of rectangular cross section (DNV-RP-C205, 2010)

Plane shape	l/w	b/d	Drag coefficient for h/b ratio				
			Up to 1	1	2	4	6
	≥ 4	≥ 4	1.2	1.3	1.4	1.5	1.6
		$\leq 1/4$	0.7	0.7	0.75	0.75	0.75
	3	3	1.1	1.2	1.25	1.35	1.4
		1/3	0.7	0.75	0.75	0.75	0.8

For the pontoon structure, the drag coefficient (C_D) will be equal to 1.156.

5.8.2 Wind Drag Coefficient Calculation

The drag force acting on large structures can be approximated by,

$$F_j(\beta) = C_{dj}(\beta)|u|u \text{ where } j = 1, 6 \quad (22)$$

Where, j (1,3) : force component in local (x,y,z) direction

j (4,6) : moment component about local (x,y,z) direction

C_{dj} : Wind drag coefficient in jth direction

u : Relative wind velocity in the wind direction

For the floating structure, in time domain simulation the relative heading angle of wind and structure will vary continuously, and required to input the drag force in range of relative heading angle. In ANSYS Aqwa, the drag forces are input as

$$C_{dj}(\beta) = \frac{F_{j\beta}}{u^2} \quad (23)$$

Table 5: Wind drag coefficient

Direction	X(N/(m/s) ²)	Y(N/(m/s) ²)	Z(N/(m/s) ²)	RX(Nm/(m/s) ²)	RY(Nm/(m/s) ²)	RZ(Nm/(m/s) ²)
-180	-282.1	0	0	0	-5159	0
-135	-197.9	-197.9	0	3635	-3635	0
-90	0	-282.1	0	5159	0	0
-45	197.9	-197.9	0	3635	3635	0
0	282.1	0	0	0	5159	0
45	197.9	197.9	0	-3635	3635	0
90	0	282.1	0	-5159	0	0
135	-197.9	197.9	0	-3635	-3635	0
180	-282.1	0	0	0	-5159	0

The drag forces in intermediate angle will be interpolated by the software.

5.8.3 Response Analysis for Maximum Regular Wave Height

Regular wave ULS has been applied on the structure in 0 - and 45-degrees heading angles. As per design criteria, maximum angle with vertical, maximum and minimum accelerations, tension in the mooring cables, air-gap between wave elevation and cable deck, relative distance between bottom and wave elevation (bottom emergence check) are checked.

5.8.3.1 Tension on Mooring Lines

In all the time of the operation of the TLP platform, the force in the cable should be +ve (should never slack).

The tension in the mooring lines is studied for different angle of incident of wave and wind and found that the maximum tension in the mooring line will be when the load is at 45 degrees to the platform.

From the response results (the results are not shown due to confidentiality nature of the report), It is clear that the tension on the mooring line is always positive and not slacking.

It is clear that, the maximum tension is on the mooring line 4. This maximum load should be the design load for all the tendons, because the direction of waves and wind can be from any side/angle around the structure.

$$\begin{aligned} \text{The maximum stress on the mooring lines, } \sigma &= \frac{\text{Maximum tension (N)}}{\text{Cross-section area (mm}^2\text{)}} = \frac{19452520}{\pi * (0.15)^2} = \\ &= 275 \text{ N/mm}^2 \end{aligned}$$

The allowable stress for the mooring line is 235 N/mm². To reduce the stress on each mooring line, additional mooring lines are added on each corner with same initial mooring line property. It will change the unstretched length of cable as 184.93m as per the calculation shown in section 5.6.1 and resulting tension on one cable will be half of the tension. To find the tension on each mooring lines, simulation is carried out for added mooring stiffness.

From the results, It is clear that the tension is always positive and no slack of mooring lines for the new configuration. And the maximum tension is 19386542 N at mooring line 4. So, the tension on one mooring line will be half (9693271 N). And the stresses on one mooring line will 137.13 N/mm² which is acceptable (<235 N/mm²).

5.8.3.2 Maximum Angle with Vertical

To avoid the fouling between the cable and structure, maximum angle of the cable with the vertical axis is restricted to 30 deg.

The offset is greater for the 45-degree case compared to 0-degree wave heading case. The offset in the direction of the wave heading will be maximum. To find the resultant offset distance for 45 degree wave heading case, Eq. (24) can be used.

The maximum offset is 22.1 meter. So the angle of the cable with the vertical axis will be $\tan^{-1} \frac{22.1}{200} = 6.3 \text{ deg.}$ (where, 200m is the depth of the sea bed). The angle is within the limit (< 30 deg).

5.8.3.3 Acceleration

To reduce the design load of the structure and equipment, the acceleration value should be in limited values. Also, the less acceleration will help to reduce the sea sickness due to the motion of the structure.

The maximum and minimum values of the accelerations for all 6 degrees of freedom at center of gravity of the structure have to be evaluated. The values are not given in the report due to the confidentiality reason. The accelerations are within the limits.

5.8.3.4 Minimum Air gap

Minimum air-gap between cable deck and wave elevation should be positive value in order to avoid the deck slamming.

From the analysis, it is clear that the wave elevation and position on the deck are not crossing. The minimum air-gap between cable deck and wave elevation is 1.46m.

5.8.3.5 Check for Bottom Emergence

As a design check, the bottom of the platform should not emerge out of the water.

The minimum distance between bottom point and wave elevation is 11.27m. It means, the pontoon structure always will be below the wave elevation.

5.8.4 Response Analysis for Irregular Wave (ULS)

For the TLP platform, a sea state of 100-year return period ($H_s=13.54$ m, $T_p=13.89$ s in 0 deg and +45 deg) is used for the simulation (as discussed in section 5.2.2). Normally, it is assumed that simulated irregular sea states are stationary about 3 hours (DNV-RP-C205, 2010). As the spectrum of the wave represent for 3 hours of wave data, the response simulation time should be 3 hours (10800 sec).

As per design criteria, maximum angle with vertical, maximum and minimum accelerations, tension in the mooring cables, air-gap between wave elevation and cable deck, relative distance between bottom and wave elevation (bottom emergence check) are checked. All criteria are within the limit except the air-gap between wave elevation and topside bottom deck.

5.8.4.1 Minimum Air gap

The relative distance between wave elevation and cable deck (air gap) should be greater than zero to avoid the slamming. The negative value means the wave elevation is crossing the cable deck height which is not acceptable.

A negative value of 3.1m is obtained after the analysis. It means, the wave will reach above 3.1 m of cable deck. To avoid this, the height of cable deck has to be increased by 4m.

5.8.4.2 Response Analysis for Modified TLP platform

Due to increase in the height of the top side, the mass properties of the structure will change. Also, wind drag force will be increased due to the height increase. The modified mass properties cannot shown in this report due to confidential nature of the report.

The new wind drag coefficients are given in Table 6.

Table 6: Drag coefficient for new structure

Direction	X(N/ (m/s)²)	Y(N/ (m/s)²)	Z(N/ (m/s)²)	RX(Nm/ (m/s)²)	RY(Nm/ (m/s)²)	RZ(N m/ (m/s)²)
-180	-299	0	0	0	-5475	0
-135	-209.7	-209.7	0	3855.2	-3855.2	0
-90	0	-299.5	0	5475	0	0
-45	209.7	-209.7	0	3855.2	3855.2	0
0	299	0	0	0	5475	0
+45	209.7	209.7	0	-3855.2	3855.2	0
+90	0	299	0	-5475	0	0
+135	-209	209	0	-3855	-3855	0
+180	-299	0	0	0	-5475	0

5.8.4.2.1 Air gap

The air gap is less for the Irregular wave ULS case for the heading angle 45 degree compared to 0 degree. After the analysis, it is clear that the minimum air gap is greater than zero (1.02m) in all simulation time for the modified structure.

5.8.4.2.2 Tension on Mooring Lines

Maximum and minimum tension on the mooring lines for 0 deg and 45 deg irregular waves ULS case are tabulated in Table 7.

Table 7: Mooring line tension for irregular wave case – For modified structure

	0 deg. Irregular wave		45 deg. Irregular wave	
Mooring line	Tension _Max. (N)	Tension_Min. (N)	Tension _Max. (N)	Tension_Min. (N)
Mooring line 1	17536314	4666418	17978446	4277149
Mooring line 2	17550730	4656807	18913172	4851441
Mooring line 3	21361720	1129359	17964028	4277149
Mooring line 4	21347320	1179820	22942822	4811249

It is clear that, the maximum tension is on the mooring line 4 which is for Irregular wave ULS 45 deg heading case. This maximum tension should be the design load for all the tendons, because the direction of waves and wind can be from any side/angle around the structure. As each mooring cable in the model stands for two mooring lines, the maximum tension on one mooring line will be 11471411 N.

$$\begin{aligned} \text{The maximum stress on the mooring lines, } \sigma &= \frac{\text{Maximum tension (N)}}{\text{Cross-section area (mm}^2\text{)}} = \frac{11471411}{\pi * (0.15)^2} = \\ &= 162.2 \text{ N/mm}^2 \end{aligned}$$

The stresses on the mooring lines are within acceptable limits (< 235 N/mm²).

5.8.4.2.3 Accelerations

Maximum and minimum accelerations of the modified structure for 0 deg and 45 deg irregular waves ULS case are evaluated after the analysis and noticed that the results are within the limits.

5.8.4.2.4 Maximum Angle with Vertical

The maximum offset for 45 deg Irregular wave case will be in the direction of wave heading. To calculate the offset, following equation need to be used;

$$\text{Max.offset for 45 deg case at time, } t = \sqrt{\text{Surge}(t)^2 + \text{sway}(t)^2} \quad (24)$$

The maximum offset for the irregular case with wave heading 45 degree is within the limits.

5.8.4.2.5 Check for Bottom Emergence

Relative distance between wave surface elevation and bottom point is checked. The minimum relative distance between wave surface elevation and bottom point is 10.2 m and it is evident that the pontoon structure is below water in all the case.

5.9 Cable Lay-outing

Due to the limited capabilities of the ANSYS Aqwa on electrical cable modelling and analysis, only two cabling lay-outing were checked around the floating substation – catenary and lazy wave shape having same length and properties. The tension at the connection of floater were checked for Irregular wave ULS (with 45 degrees heading angle) condition as explained in section 5.2.2. The cable lay-out with less tension on the connection of floater were chosen as final layout.

5.9.1 Cable and Buoy properties

To get proper support for the cables, all the cables are running through the vertical column from cable deck to bottom of TLP platform. At each vertical column two cables are considered in X and Y direction for both cable arrangement (catenary and lazy wave). The cable properties used for the simulation are tabulated in Table 8.

Table 8: Electrical cable and Buoy properties

Properties	Values
Cable diameter (mm)	61.5
Weight in air (kg/m)	9.11
Weight in sea water (kg/m)	6.06
Axial stiffness (MN)	66
Bending stiffness (Nm ²)	1560
Maximum tension (kN)	15
Buoy weight (kg)	50
Displaced mass of Buoy (kg)	250

5.9.2 Cable Arrangement and Shapes

The cable shape dimensions for both the layout are shown in Figure 24 and Figure 25.

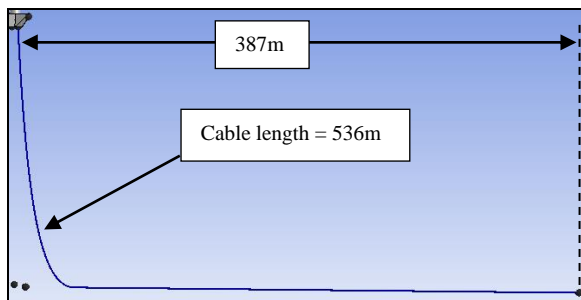


Figure 24: Catenary shape-dimensions

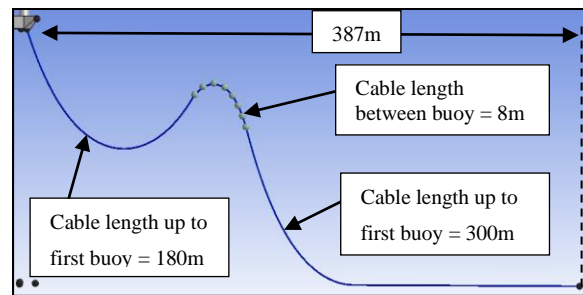


Figure 25: Lazy wave shape-dimensions

5.9.3 Cable Tension

To find the best cable layout in the point of less tension, the Irregular wave ULS with 45-degree heading (as per section 5.2.2) has been applied to the structure for both the

arrangement. The tension of the electrical cables at the connection with floater will be maximum and tabulated in Table 9.

Table 9: Maximum and minimum tension of cables at the floater connection

Mooring line	Catenary shape		Lazy wave shape	
	Tension_Max. (N)	Tension_Min. (N)	Tension_Max. (N)	Tension_Min. (N)
Cable 1	14052	5632	10539	3121
Cable 2	14053	5653	10529	3115
Cable 3	16285	5318	10927	2478
Cable 4	14055	5651	10529	3115
Cable 5	16300	5308	10926	2476
Cable 6	16298	5301	10931	2471
Cable 7	16298	5312	10926	2477
Cable 8	14061	5620	10538	3114

From Table 9, it is clear that the maximum tension is for the catenary shape in all the cable. This is due to the fact that, for lazy wave shape buoy will support some part of the weight of the cable and reduces the tension at the floater connection. Also, for catenary shape arrangement, the probability to hit the cable on mooring line is high. Due to this reasons, best layout is lazy wave shape compared to catenary shape.

6 CONCLUSION

Through this report, the state-of-the-art review of AC/DC Tension Leg Platform (TLP) cable lay-outing and hydrodynamic modelling & analysis of the GICON AC/DC TLP platform using potential solver, ANSYS Aqwa have been done. GICON AC/DC TLP platform is designed by the conversion of existing GICON O&M Platform. The platform was analyzed for two Ultimate Limit Cases (ULS) – 100-year return period regular ($H_{max}=25.26$ m, $T=13.89$ s) and irregular ($H_s=13.54$ m, $T_p=13.89$ s) waves at North Atlantic Sea having 200m water depth case. Both the waves are analyzed for heading angles 0 degree and 45 degree to the TLP structure. The structure shows the maximum response to the Irregular wave condition at 45 degrees heading.

The mass properties of the platform are calculated using the software, SOLIDWORKS. The drag forces are approximated using analytical equations as per DNV-RP-C205 (DNV-RP-C205, 2010). The stress developed on mooring lines for regular wave ULS at 45 degree heading overcame the stress limit of the mooring lines. Initially the number of mooring lines were 4 (one at each corner) and to reduce the stress on mooring lines one mooring is added at each corner of the TLP platform. The stress on mooring lines are reduced for all ULS cases.

To avoid the deck slamming, the air gap between cable deck and waterline is analyzed. Air gap were less than zero for all the irregular wave conditions. To avoid this, entire topside height including cable deck of the TLP platform is increased by 4m.

The angle of the mooring lines with vertical, maximum tension on mooring lines, relative distance between wave surface and cable deck, relative distance between wave surface and bottom of the pontoon are checked for modified structure with irregular wave ULS conditions. All the results were satisfactory for the new TLP platform (with added mooring line and increased depth).

Two basic configurations of electrical cable were modelled – catenary and lazy wave shape. Cable tension at the connection of platform with electrical cable due to the motion of the floating structure for Irregular wave ULS with heading angle 45 degree is analyzed and

compared the results. The cable layout chosen for GICON AC/DC TLP is lazy wave shape due to its less tension and less probability to hit on mooring lines compared to catenary shape.

7 FUTURE WORK

This study is only concerned about the hydrodynamic analysis of the AC/DC TLP platform for only one load case in severe operation condition – 100-year return period load case (Ultimate Load Case). To finalize the design, a number of additional load cases has to be checked before finalizing the TLP design. Some of the future work to accomplish the complete design in hydrodynamic aspects are listed below:

- Structural strength calculations.
- Stability analysis of the modified platform (intact and damage) in all conditions.
- Hydrodynamic analysis of TLP in operation, installation and transportation conditions.
- Hydrodynamic analysis of the Platform in accidental load cases (like damage of mooring lines).
- Modelling and analyze the dynamic cables (electrical cables) with bending stiffener, bending resistor..etc.
- Fatigue strength evaluation of the cables.
- Computational Fluid Dynamics (CFD) simulation to find current and wind drag forces on the structure.
- Comparison of the potential solver results to the model test.

8 ACKNOWLEDGEMENT

I am highly grateful to my parents to give me guidance and support in life to make me accomplish and chase my dreams.

I sincerely extend my gratitude to Dr. Frank Adam, Hartmann Hauke and Johannes Wahrendorf from Großmann Ingenieur Consult GmbH (GICON), Rostock to give the opportunity to work on the master thesis, guiding me, supporting me to complete the master thesis work. I am thankful to Prof. Guillaume Ducrozet, Prof. Felicien Bonnefoy, Prof. Lionel Gentaz and Prof. Pierre Ferrant and all the professors from Ecole Centrale Nantes, France who helped me for explaining in-depth concepts of hydrodynamics. I am thanking to the Prof. Philippe Rigo and all professors from University of Liege for all the support throughout the master course for sharing and imparting their valuable knowledge in their field of expertise.

9 REFERENCE

ANSYS, 2013. *Aqwa theory manual*. s.l.:s.n.

Bachynski, E. E. & Moan, T., 2012. Design considerations for tension leg platform wind turbine. *Marine Structures*, September, Volume 29, pp. 89-114.

Binbin, L., 2011. Hydrodynamic Comparison of a Semi-submersible, TLP, and Spar: Numerical Study in the South China Sea Environment. *Marine Science and Application*, September , Volume 10, pp. 306-314.

DNVGL-ST-0359, June, 2016. *Subsea power cables for wind power plants*. s.l.:s.n.

DNV-RP-C205, R. P., 2010. *ENVIRONMENTAL CONDITIONS AND ENVIRONMENTAL LOADS*. s.l.:s.n.

DNV-RP-J301, 2016. *Subsea Power Cables in Shallow Water Renewable Energy Applications*. s.l.:s.n.

Kim, C.-H., Lee, C.-H. & Goo, J.-S., 2007. A dynamic response analysis of tension leg platforms including hydrodynamic interaction in regular waves. February, Volume 34, pp. 1680-1689.

Rentschler, M. U. T. et al., 2020. Parametric study of dynamic inter-array cable systems for floating offshore wind turbines. 8 January, Volume 15, pp. 16-25.

TANINOKI, R., 2017. *Dynamic Cable System for Floating Offshore Wind Power Generation*. s.l.:s.n.

W.-S.Moon, J.-C. K. A. J.-N. W., 2014. *Grid optimization for ofshore wind farm layout and substation location, in ITEC Asia-Pacific 2014*. Beijing, s.n.

Zhao, S. et al., 2021. A comparison of two dynamic power cable configurations for a floating offshore wind turbine in shallow water. 7 February.